PROCEEDINGS OF THE ROYAL SOCIETY A

rspa.royalsocietypublishing.org

Research

Cite this article: Ciambella J, Saccomandi G. 2014 A continuum hyperelastic model for auxetic materials. *Proc. R. Soc. A* **470**: 20130691. http://dx.doi.org/10.1098/rspa.2013.0691

Received: 16 October 2013
Accepted: 13 December 2013

Subject Areas:
materials science, mechanical engineering, applied mathematics

Keywords:
nonlinear elasticity, Poisson's ratio, foams, large strain

Author for correspondence:
J. Ciambella
e-mail: jacopo.ciambella@uniroma1.it

A continuum hyperelastic model for auxetic materials

J. Ciambella[1,2] and G. Saccomandi[3]

[1]Advanced Composites Centre for Innovation and Science, University of Bristol, Bristol BS8 1TR, UK
[2]Dipartimento di Ingegneria Strutturale e Geotecnica, Sapienza Università di Roma, Rome 00184, Italy
[3]Dipartimento di Ingegneria Industriale, Università degli Studi di Perugia, Perugia 06125, Italy

We propose a simple mathematical model to describe isotropic auxetic materials in the framework of the classical theory of nonlinear elasticity. The model is derived from the Blatz–Ko constitutive equation for compressible foams and makes use of a non-monotonic Poisson function. An application to the modelling of auxetic foams is considered and it is shown that the material behaviour is adequately described with only three constitutive parameters.

1. Introduction

Poisson's ratio, i.e. minus the ratio between perpendicular strain over the tensile strain in the stretching direction, is one of the two constitutive coefficients needed to characterize linear isotropic elastic materials [1]. For *standard* materials (for example, steels or plastics), Poisson's ratio has a positive value, ideal incompressible rubber has a Poisson ratio of 0.5 and ideal cork a ratio of 0. Most naturally occurring materials have Poisson's ratio values ranging between 0.0 and 0.5, but some denoted as *auxetic* display a negative Poisson ratio: when subjected to a simple tension, they undergo lateral expansion and lateral compression when compressed. Natural occurring materials showing this effect are, for instance, silicate [2], some polymeric systems [3] and zeolites [4]. This behaviour is exactly the opposite one would expect when testing standard materials under uniaxial tension.

Although the theoretical possibility of having a Poisson ratio less than zero has been known for centuries, it was only at the end of the last century that auxetic materials were actually manufactured [5]. In 1987, a conventional foam was converted to auxetic by

exploiting a re-entrant honeycomb cell structure [6]; the resulting material was isotropic with a Poisson ratio of −0.7. Over the years, the manufacturing techniques have been refined and different material properties have been achieved by controlling the re-entrant cell shape [7,8].

In the linear theory of elasticity, the auxetic effect is easily accounted for with a negative Poisson ratio. Homogenized models able to describe the relationship between the foam microstructure and the constitutive constants have been adopted (for instance [9–11]); these models are based on a kinematic map between displacements/rotations at the cell level and the deformation at the macroscale; as such, they are strictly dependent on the microstructure of the foam. Furthermore, being limited to small strains, they are not able to describe the dependence between the lateral expansion and stretch seen in the experimental data. For these reasons, nonlinear elastic models have to be considered.

In the nonlinear theory of elasticity, the constitutive constants play a complete different role than they do in the linear theory. Indeed, these coefficients cannot be used to represent the mechanical properties of nonlinear elastic materials as the response is in general described by constitutive functions [12]. Murphy [13] and Murphy & Rogerson [14] have shown that a simple tension test is sufficient to characterize the mechanical behaviour only of the special class of compressible isotropic hyperelastic materials whose strain energy function has the form $W = \hat{W}(J_1 - k_1(J_3), J_2 - k_2(J_3))$, where J_1, J_2 and J_3 are independent invariants of the left Cauchy–Green strain tensor and k_1 and k_2 are two functions of J_3. This is an important class of materials as they contain the well-known constitutive equation proposed by Blatz & Ko [15].

In this constitutive framework, we show that the idea behind the Blatz–Ko model can be extended to describe auxetic materials, provided that a proper Poisson function is chosen. To the best of our knowledge, for the first time, we provide a constitutive setting to model in the framework of continuum nonlinear elasticity materials which undergo lateral expansion when subjected to a simple tension and lateral compression when compressed.

We use the proposed constitutive equation to explain some experimental data on Scott's foams by Lakes and co-workers [16]. These data, shown in figures 8–10, are indeed representative of a large class of auxetic materials as a similar behaviour has been observed in open cell-compliant polyurethane foams [7], chiral honeycombs [17] and even in warp knit auxetic fabrics [18].

The plan of the paper is as follows: in the next section, we write down the basic equations and we introduce and discuss the auxetic Poisson function. In §3, we show that the Blatz–Ko model can account for the auxetic effect but it has some limitations in describing the experimental data. The proposed constitutive model is presented in §4 and compared to the experimental data in §5. Finally, recommendations for further work are made in §6.

2. Basic equations

Let $\mathbf{x}$ denote the current position of a particle $\mathbf{X}$ in the reference configuration that is assumed to be stress free. The motion of the body is a one to one mapping $\chi(\mathbf{X}, t)$ that assigns to each point $\mathbf{X}$ belonging to the reference configuration the position $\mathbf{x}$ at time t, i.e. $\mathbf{x} = \boldsymbol{\chi}(\mathbf{X}, t)$. The displacement $\mathbf{u}$ and deformation gradient $\mathbf{F}$ are defined through $\mathbf{u} = \mathbf{x} - \mathbf{X}$ and $\mathbf{F} = \partial\boldsymbol{\chi}/\partial\mathbf{X}$. The Cauchy–Green left tensor $\mathbf{B}$ is defined through $\mathbf{B} = \mathbf{F}\mathbf{F}^{\mathrm{T}}$.

For a hyperelastic material, one can postulate the existence of a strain energy function W, which depends on the deformation tensor $\mathbf{B}$. Additionally, if the material is isotropic, the dependence of W on $\mathbf{B}$ is only through the principal invariants, i.e. $W = W(J_1, J_2, J_3)$ with

$$J_1 = \operatorname{tr}\mathbf{B}, \quad J_2 = \operatorname{tr}\mathbf{B}^{-1} \quad \text{and} \quad J_3 = \det\mathbf{F}. \tag{2.1}$$

The Cauchy stress can be expressed in terms of the derivative of the strain energy function as

$$\boldsymbol{\sigma} = \frac{\partial W}{\partial J_3}\mathbf{I} + \frac{2}{J_3}\frac{\partial W}{\partial J_1}\mathbf{B} - \frac{2}{J_3}\frac{\partial W}{\partial J_2}\mathbf{B}^{-1}. \tag{2.2}$$

The mechanical characterization of auxetic materials is normally carried out through simple tension/compression experiments. It is well known that for linear elasticity a simple tension

produces a simple extension provided that the shear modulus $\mu_0 \neq 0$ or ∞ and that the simple tension experiment is sufficient to determine directly Young's modulus

$$E = \mu_0 \frac{3\bar{\lambda} + 2\mu_0}{\bar{\lambda} + \mu_0}$$

and Poisson's ratio

$$\nu_0 = \frac{1}{2} \frac{\bar{\lambda}}{\bar{\lambda} + \mu_0},$$

where μ_0 and $\bar{\lambda}$ are the so-called Lamé moduli.

From these formulae and stability consideration, one obtains the well-known range of Poisson's ratio, i.e. $-1 < \nu_0 \leq 1/2$, valid for isotropic free-standing solids in three dimensions [1]. As such, one is able to characterize (via a standard experiment) in a complete way any material modelled as isotropic and linear elastic.

In the nonlinear theory of elasticity, the situation is much more complex. In this framework, Batra [19] showed that a simple tensile loading, i.e.

$$\boldsymbol{\sigma} = \mathrm{Diag}(0, 0, T) \tag{2.3}$$

corresponds uniquely, in the family of homogeneous deformations, to an extensional deformation $\lambda_1 = \lambda_2$, $\lambda_3 = \lambda$, i.e.

$$\mathbf{B} = \mathrm{Diag}(\lambda_1^2, \lambda_1^2, \lambda^2), \tag{2.4}$$

if the empirical inequalities $\partial W/\partial J_1 > 0$, $\partial W/\partial J_2 \geq 0$ hold. We point out that the remaining empirical inequality proposed by Truesdell & Noll [20], i.e. $\partial W/\partial J_3 \leq 0$, is not necessary to achieve Batra's results. In the previous equation, λ is the stretch in the direction of the tensile force, i.e. $\lambda := \ell/\ell_0$, and λ_1 and λ_2 are the stretches in the orthogonal directions.

From (2.2) to (2.4), one has that the following equations must hold in order to satisfy the boundary conditions for the simple tensile loading:

$$T = \frac{\partial W}{\partial J_3} + \frac{2}{J_3}\frac{\partial W}{\partial J_1}\lambda^2 - \frac{2}{J_3}\frac{\partial W}{\partial J_2}\lambda^{-2} \tag{2.5}$$

and

$$0 = \frac{\partial W}{\partial J_3} + \frac{2}{J_3}\frac{\partial W}{\partial J_1}\lambda_1^2 - \frac{2}{J_3}\frac{\partial W}{\partial J_2}\lambda_1^{-2}, \tag{2.6}$$

where $J_1 = \lambda^2 + 2\lambda_1^2$, $J_2 = \lambda^{-2} + 2\lambda_1^{-2}$ and $J_3 = \lambda\lambda_1^2$.

In general, (2.5) and (2.6) cannot be solved until constitutive assumptions on the strain energy function and on the relationship between λ_1 and λ are made.

For an incompressible material, for instance, one has

$$\lambda_1 = \lambda^{-1/2}, \tag{2.7}$$

which follows from the incompressibility constraint $J_3 = 1$.

In the general case of unconstrained solids, one can assume that λ_1 is a continuous function of λ, i.e.

$$\lambda_1 = g(\lambda), \tag{2.8}$$

or equivalently one can define the ratio between lateral and longitudinal strains

$$\nu(\lambda) := -\frac{\lambda_1 - 1}{\lambda - 1} = -\frac{g(\lambda) - 1}{\lambda - 1}, \tag{2.9}$$

or the volume variation

$$J_3 := \lambda_1^2\lambda = g(\lambda)^2\lambda. \tag{2.10}$$

All these definitions are, indeed, equivalent ways to express the relationship between the longitudinal and lateral stretches; it may be preferable to use one over the other regarding the type of experimental data available.

The function $\nu(\lambda)$ in (2.9) is an extension of Poisson's ratio ν_0 to large strain and is known as *Poisson's function* [12]; indeed, $\nu(\lambda) \to \nu_0$ for $\lambda \to 1$. When $\nu(\lambda) < 0$, the material displays the auxetic effect sought after.

In the following, it is assumed that the strain energy function W can be split as the sum of two terms,

$$W(J_1, J_2, J_3) = W_3(J_3) + W_{12}(J_1, J_2), \tag{2.11}$$

with W_3 dependent on J_3 alone. This is indeed a common assumption satisfied by several well-known models.

By substituting (2.6) into (2.5), one obtains the following set of equations:

$$T = \frac{2}{J_3}\frac{\partial W_{12}}{\partial J_1}(\lambda^2 - \lambda_1^2) - \frac{2}{J_3}\frac{\partial W_{12}}{\partial J_2}(\lambda^{-2} - \lambda_1^{-2}) \tag{2.12}$$

and

$$\frac{\partial W_3}{\partial J_3} = -\frac{2}{J_3}\frac{\partial W_{12}}{\partial J_1}\lambda_1^2 + \frac{2}{J_3}\frac{\partial W_{12}}{\partial J_2}\lambda_1^{-2}. \tag{2.13}$$

Assuming that relationship (2.10) between J_3 and λ is invertible, say $\lambda = h(J_3)$, equation (2.13) can be rewritten in terms of J_3 only. In this situation, one can integrate (2.13) and obtain the expression of $W_3(J_3)$. However, $h(J_3)$ can be calculated in closed form only in very special cases (see [14]).

Two equations (2.12) and (2.13) show that the strain energy function can be obtained from the experimental data with the following steps:

(i) Determine from the experiments the relationship between longitudinal stretch and λ, or equivalently Poisson's function.
(ii) Identify from the stress–strain curves the constitutive functions $\partial W_{12}/\partial J_1$ and $\partial W_{12}/\partial J_2$ through equation (2.12).
(iii) Integrate equation (2.13) to obtain the strain energy function $W_3(J_3)$.

We remark that the previous steps are indeed independent of the choice of the strain energy function provided that equation (2.11) is valid. In the following, we restrict ourselves to the case of a linear dependence of W_{12} on J_1 and J_2, i.e.

$$W_{12} = \frac{\mu_0}{2} f(J_1 - 3) + \frac{\mu_0}{2}(1 - f)(J_2 - 3). \tag{2.14}$$

Despite its simplicity, this form of the strain energy function has been successfully used to model a wide class of materials, including elastomers, composites, soft-tissues and foams, and corresponds to Mooney–Rivlin and Blatz–Ko compressible models.

It is seen from equation (2.14) that the resulting constitutive equation satisfies the empirical inequalities $\partial W_{12}/\partial J_1 > 0$ and $\partial W_{12}/\partial J_2 \geq 0$, if and only if $\mu_0 > 0$ and $0 < f \leq 1$. The third empirical inequality [20], i.e. $\partial W_3/\partial J_3 \leq 0$ is in general not satisfied, in fact,

$$\frac{\partial W_3}{\partial J_3} = -\frac{\mu_0}{J_3} f\lambda_1^2 + \frac{\mu_0}{J_3}(1 - f)\lambda_1^{-2} \leq 0 \quad \Longleftrightarrow \quad \lambda_1^2 \geq \sqrt{\frac{1-f}{f}}. \tag{2.15}$$

In the underformed configuration ($\lambda = \lambda_1 = 1$) $\partial W_3/\partial J_3 \leq 0$ if and only if $1/2 \leq f \leq 1$; if $f = 1$, the empirical inequality (2.15) holds true for every λ_1.

With the strain energy (2.14), equations (2.12) and (2.13) simplify into

$$\frac{\partial W_3}{\partial J_3} + \frac{\mu_0 f}{J_3}\lambda_1^2 - \mu_0\frac{1-f}{J_3}\lambda_1^{-2} = 0 \quad \text{and} \quad T = \frac{\partial W_3}{\partial J_3} + \frac{\mu_0 f}{J_3}\lambda^2 - \mu_0\frac{1-f}{J_3}\lambda^{-2}. \tag{2.16}$$

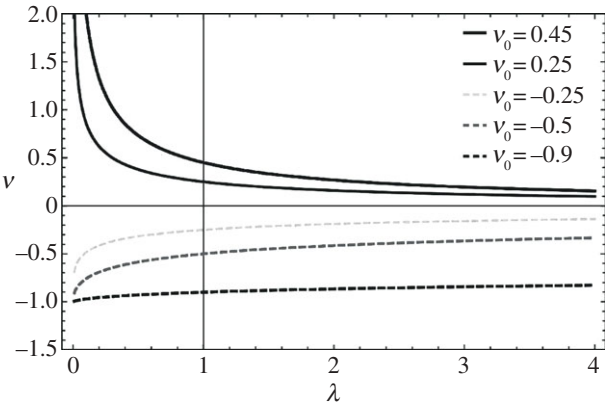

Figure 1. Poisson's function ν of the Blatz–Ko model (equation (3.2)) for positive and negative values of the infinitesimal Poisson ratio ν_0. For $\nu_0 < 0$, the model displays the 'auxetic' effect.

3. Blatz–Ko auxetic model

The main idea of the celebrated Blatz–Ko paper [15] is to consider the following relationship between lateral and longitudinal stretch:

$$\lambda_1 = \lambda^{-\nu_0}, \tag{3.1}$$

where ν_0 (the infinitesimal Poisson ratio) has to be determined by the experimental tests. The corresponding Poisson function is

$$\nu(\lambda) = \frac{1-\lambda^{-\nu_0}}{\lambda - 1} \tag{3.2}$$

and

$$J_3(\lambda) = \lambda^{1-2\nu_0}, \tag{3.3}$$

which is a continuous monotonic, thus invertible, function.

It is easy to check that if $\nu_0 > 0$, (3.2) is a positive function and if $\lambda > 1$ then $\lambda_1 = \lambda_2 < 1$ (see (3.1)). On the contrary, if $\nu_0 < 0$ then (3.2) is a *negative* function and from (3.1) we have that if $\lambda > 1$ then $\lambda_1 = \lambda_2 > 1$, which corresponds to the lateral expansion observed in auxetic materials.

The Blatz–Ko's function $\nu(\lambda)$ is plotted in figure 1 for different values of the infinitesimal Poisson ratio ν_0. For $\nu_0 > 0$, $\nu(\lambda)$ has a vertical asymptote at $\lambda = 0$ and monotonically decreases to 0. For $\nu < 0$, it achieves the minimum at $\lambda = 0$ ($\nu(0) = -1$) and then monotonically increases to its horizontal asymptote at 0. The functional dependence for $\nu_0 > 0$ has proved to be particularly effective in modelling the behaviour of certain compressible foams at large strain (see for instance [12,14]).

The class of Blatz–Ko materials (3.1) can, hence, be extended trivially to describe an auxetic material when ν_0 in (3.1) is negative.

We point out that with (3.3), the computation of the corresponding $\partial W_3/\partial J_3$ from equation (2.16) is a simple matter and it gives

$$\frac{\partial W_3}{\partial J_3} = \mu_0 J_3^{-1}\left[(1-f)J_3^{2\nu_0/(1-2\nu_0)} - f J_3^{-2\nu_0/(1-2\nu_0)}\right]. \tag{3.4}$$

To highlight the difference between the standard case $\nu_0 > 0$ and the auxetic case $\nu_0 < 0$, we now consider a deformation given by a simple shear superimposed to a triaxial extension. This problem was studied in [21] for the generalized Blatz–Ko material with $\nu_0 > 0$. The corresponding

deformation is

$$x = \lambda_1 X + K\lambda_2 Y, \quad y = \lambda_2 Y \quad \text{and} \quad z = \lambda_3 Z, \tag{3.5}$$

where K is the amount of shear and λ_i $(i = 1, 2, 3)$ are the stretches associated with the triaxial extension. Under this deformation, a square in the X, Y-plane is transformed into a parallelogram in the x, y-plane. If we confine ourselves to the case $\lambda_3 = 1$ ($J_3 = \lambda_1\lambda_2$) and we require that both σ_{22} (normal traction on the top side of the parallelogram) and the traction on the slanted side of the parallelogram are null, we have to determine λ_1 and λ_2 from the equations [21]

$$\lambda_1^2 = \lambda_2^2(1 + K^2) \tag{3.6}$$

and

$$f\lambda_1^2\lambda_2^3[\lambda_1 + \lambda_2 h(\lambda_1\lambda_2)] + h(\lambda_1\lambda_2)(f - 1)[\lambda_1\lambda_2 h(\lambda_1\lambda_2) - K^2\lambda_2^2 - \lambda_1^2] = 0, \tag{3.7}$$

where we have used the inverse function of (2.10), i.e. $h(J_3)$.

For $f = 0$, the solution of (3.6) and (3.7) is given by

$$\lambda_1^2 = \lambda_2^2(1 + K^2) \quad \text{and} \quad \lambda_1^2 + K^2\lambda_2^2 - \lambda_1\lambda_2 h(\lambda_1\lambda_2) = 0. \tag{3.8}$$

By using equation (2.10), and by substituting the first equation into the second, we obtain

$$\lambda_1 = \sqrt{1 + 2K^2}\, g\left(\frac{1 + 2K^2}{\sqrt{1 + K^2}}\right), \quad \lambda_2 = \sqrt{\frac{1 + 2K^2}{1 + K^2}}\, g\left(\frac{1 + 2K^2}{\sqrt{1 + K^2}}\right), \tag{3.9}$$

in terms of the function g in (2.8).

For $f = 1$, the solution of (3.6) and (3.7) is computed from

$$\lambda_1^2 = \lambda_2^2(1 + K^2) \quad \text{and} \quad \lambda_1 - \lambda_2 h(\lambda_1\lambda_2) = 0, \tag{3.10}$$

and one obtains

$$\lambda_1 = \sqrt{1 + K^2}\, g(\sqrt{1 + K^2}) \quad \text{and} \quad \lambda_2 = g(\sqrt{1 + K^2}). \tag{3.11}$$

Once λ_1 and λ_2 are calculated, the normalized shear stress is

$$\hat{\sigma}_{12} := \frac{\sigma_{12}}{\mu_0} = K\left(f\frac{\lambda_2}{\lambda_1} + \frac{(1 - f)}{\lambda_1^3\lambda_2}\right), \tag{3.12}$$

which may be expressed as the function of the amount shear only. From simple computations, we have that the case $f = 1$ is of no interest because in this situation σ_{12} does not depend on ν_0, regardless of the constitutive choice made for λ_1. On the contrary, for $f = 0$, we obtain

$$\hat{\sigma}_{12} = K\frac{\sqrt{1 + K^2}}{(1 + 2K^2)^2}\left[g\left(\frac{1 + 2K^2}{\sqrt{1 + K^2}}\right)\right]^{-4} \tag{3.13}$$

that depends on the assumed functional dependence of the lateral stretch λ_1.

We point out that all equations (3.6)–(3.13) are valid whatever the choice of the constitutive function $g(\lambda)$ provided that equation (2.10) is invertible. For instance, for the generalized Blatz–Ko material $g(\lambda) = \lambda^{-\nu_0}$ and after a simple computation we obtain the following expression:

$$\hat{\sigma}_{12} = \mu_0 K(1 + 2K^2)^{4\nu_0 - 2}(1 + K^2)^{1/2 - 2\nu_0}, \tag{3.14}$$

plotted in figure 2. Note that, for both positive and negative ν_0, σ_{12} displays a non-monotonic response which is characteristic of the Blatz–Ko model as noted in [12]. This behaviour is not seen in the experimental data, and therefore the choice $f > 0$ is crucial in describing real-world materials.

4. Main model

The direct generalization of the Blatz–Ko idea to obtain negative Poisson's functions is trivially possible, but real-world auxetic foams have a more complex behaviour than the one described by using this machinery (see the experimental data in figure 8).

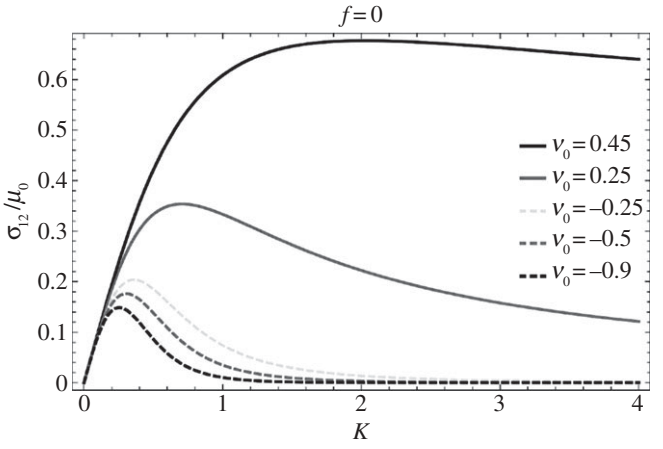

Figure 2. Normalized shear stress σ_{12}/μ_0 of the Blatz–Ko model with $f = 0$ against the shear strain K for positive and negative values of infinitesimal Poisson's ratio ν_0. For all ν_0s, $\sigma_{12}/\mu_0 \to 0$ as $K \to \infty$.

The reason why the previous approach is not sufficient to describe auxetic materials is apparent from the papers on structural aspects of auxetic foams [5,6,16,22]. Indeed, the negative Poisson ratio effect is caused by *microstructure* changes that the material undergoes when deformed. One of the best examples is the re-entrant honeycomb made of bendable ligaments proposed by Lakes [6]. When subjected to simple tension, the cells of the honeycomb unfold and then the material expands laterally. It is clear that once the unfolding of the cells has been completely achieved then the material comes back to its natural configuration and starts contracting laterally.

This behaviour can be read in a clear and neat way from the experimental data on auxetic foams [7,8], where there is a maximum stretch λ_I after which the initially auxetic material turns to be ordinary.

To model this behaviour, we have to consider a more complex Poisson function than that proposed by Blatz and Ko. A suitable choice is

$$\nu(\lambda) = \nu_0[1 + \pi^2\nu_0^2(\lambda - 1)^2]^{-q}, \tag{4.1}$$

with the corresponding lateral stretch λ_1 given by

$$\lambda_1(\lambda) = 1 - \nu_0(\lambda - 1)[1 + \pi^2\nu_0^2(\lambda - 1)^2]^{-q}. \tag{4.2}$$

In the most general case, the coefficient q is assumed to depend on the two constitutive parameters ν_0 and λ_I as follows:

$$q = \frac{1}{2} + \frac{1}{2\pi^2(\lambda_I - 1)^2\nu_0^2}, \quad q \geq \frac{1}{2},$$

which have clear physical meanings, and hence can be easily measured from experiments. In fact,

- ν_0 is the infinitesimal Poisson ratio, i.e. $\nu(\lambda) \to \nu_0$ as $\lambda \to 1$;
- λ_I is the stretch at which the material stops expanding laterally and starts contracting. This effect happens when the re-entrant facets of the microstructure responsible for the auxetic effect are completely strained.

Equations (4.1) and (4.2) are shown in figures 3 and 4 for different values of the constitutive parameters ν_0 and λ_I.

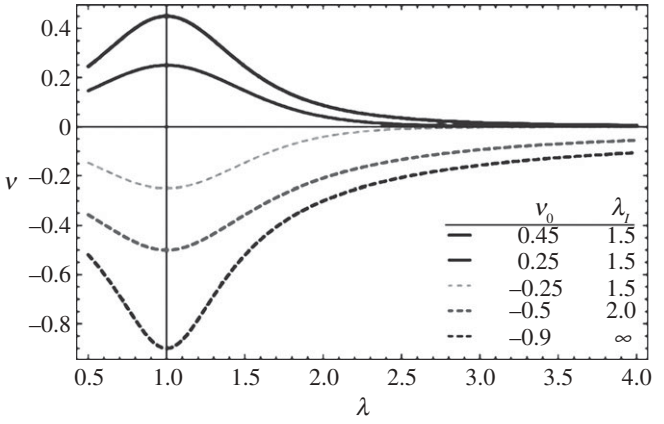

Figure 3. Functional dependence of Poisson's function ν in equation (4.1) on the longitudinal stretch λ for different values of the constitutive parameters.

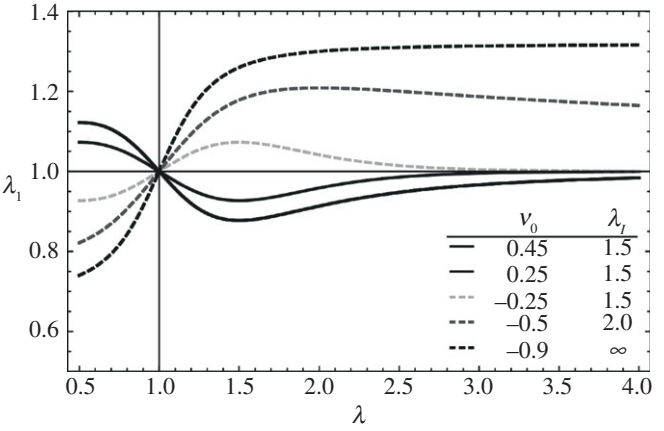

Figure 4. Lateral stretch λ_1 against longitudinal stretch λ (equation (2.8)) for different values of the constitutive parameters.

For $\nu_0 < 0$, $\nu(\lambda)$ is negative and the material displays the auxetic effect; in figure 3, the coefficient λ_I controls the velocity at which the function reaches its horizontal asymptote at 0. On the other hand, the function $\lambda_1(\lambda)$ in figure 4 increases until $\lambda = \lambda_I$ and then starts decreasing until the lateral deformation is completely recovered, i.e. $\lambda_1 \to 1$ as $\lambda \to \infty$.

For $\nu > 0$, $\nu(\lambda)$ is a positive decreasing function. More interestingly, if $\lambda < \lambda_I$ the material behaves like a 'standard' solid and it contracts laterally during the longitudinal expansion (figure 4). However, when $\lambda = \lambda_I$, the material turns out to be *slightly* auxetic and starts expanding laterally (but ν remains positive). To the best of our knowledge this behaviour has not been observed in any real material.

In both cases ($\nu \gtreqless 0$), when $\lambda_I \to \infty$ then $q \to 1/2$ and λ_1 has a horizontal asymptote at $1 + 1/\pi$ for $\nu < 0$ and at $1 - 1/\pi$ for $\nu_0 > 0$. These are upper and lower bounds for λ_1, which means that the maximum lateral deformation when this material is subjected to a simple tension loading is $1/\pi$.

Given equations (4.1) and (4.2), expression (2.10) of $J_3(\lambda)$ immediately follows, i.e.

$$J_3(\lambda) = \lambda[1 - \nu_0(\lambda - 1)(1 + \nu_0^2\pi^2(\lambda - 1)^2)^{-q}]^2. \tag{4.3}$$

For $q = 1$, $J_3(\lambda)$ is a continuous and monotonic, thus invertible, function. For $q \neq 1$, the monotonicity of $J_3(\lambda)$ cannot be proved in general but in §5 it is shown that for the corresponding

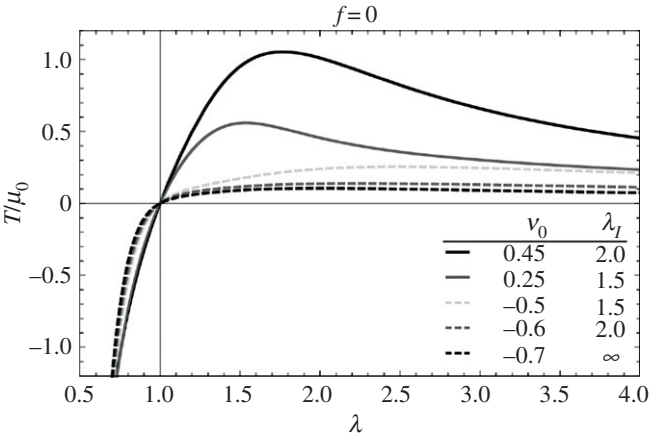

Figure 5. Normalized Cauchy stress T/μ_0 against the stretch λ for $f = 0$ and different values of the constitutive parameters λ_I and ν_0.

set of optimal parameters, equation (4.3) can be inverted. Under this circumstance, the material is said to be *simple*, according to the definition of Beatty & Stalnaker [12].

We point out that for this model the inverse function of (4.3) cannot be computed in closed form but numerically. Therefore, the solution of (2.13), thus $W_3(J_3)$, can only be obtained numerically.

By substituting (4.2) and (4.3) into (2.16), we obtain the expression of the normalized Cauchy stress in terms of λ for the simple tensile loading

$$\hat{T} := \frac{T}{\mu_0} = -\frac{f}{\lambda} - \left(\frac{1-f}{\lambda^3} - f\lambda\right)[1-(\lambda-1)\nu_0(\pi^2(\lambda-1)^2\nu_0^2+1)^{-q}]^{-2}$$

$$+\frac{1-f}{\lambda}[1-(\lambda-1)\nu_0(\pi^2(\lambda-1)^2\nu_0^2+1)^{-q}]^{-4}, \tag{4.4}$$

At small strain, the expression of Young's modulus in terms of μ_0 and ν_0 is recovered

$$E_0 = \lim_{\lambda\to 1}\frac{\partial T}{\partial \lambda} = 2\mu_0(1+\nu_0). \tag{4.5}$$

When $\nu_0 > -1/2$, Young's modulus is larger than the shear modulus as expected in standard solid materials. On the contrary for $-1 < \nu_0 \leq -\frac{1}{2}$, $E < \mu_0$, which means that the material can be more easily sheared than stretched. This behaviour is peculiar of auxetic solids.

For $f = 1$, equation (4.4) becomes

$$\hat{T} = -\frac{1}{\lambda} - \lambda[1-\nu_0(\lambda-1)(1+\pi^2\nu_0^2(\lambda-1)^2)^{-q}]^{-2}, \tag{4.6}$$

whereas for $f = 0$

$$\hat{T} = \frac{\lambda^2 - [1-\nu_0(\lambda-1)(1+\pi^2\nu_0^2(\lambda-1)^2)^{-q}]^2}{\lambda^3[1-\nu_0(\lambda-1)(1+\pi^2\nu_0^2(\lambda-1)^2)^{-q}]^4}. \tag{4.7}$$

These two relationships are plotted in figures 5 and 6 for different values of λ_I and ν_0. For $f = 1$, the effect of the microstructure changes on the overall response can be seen from the curves in figure 6. Around $\lambda = \lambda_I$, the tangent modulus slightly increases which can be seen as the re-entrant facets, responsible for the auxetic effect, being completely stretched and offering a larger resistance to the longitudinal deformation. This behaviour is indeed the opposite of what one would usually expect from a Neo-Hookean material, i.e. the case $f = 1$, that shows strain softening rather than strain hardening. Once $\lambda > \lambda_I$, the material starts acting as a 'normal' material contracting laterally instead of expanding. If further stretched, Poisson's function (4.1) assumes increasingly lower values towards 0 and the longitudinal stretch does not correspond to

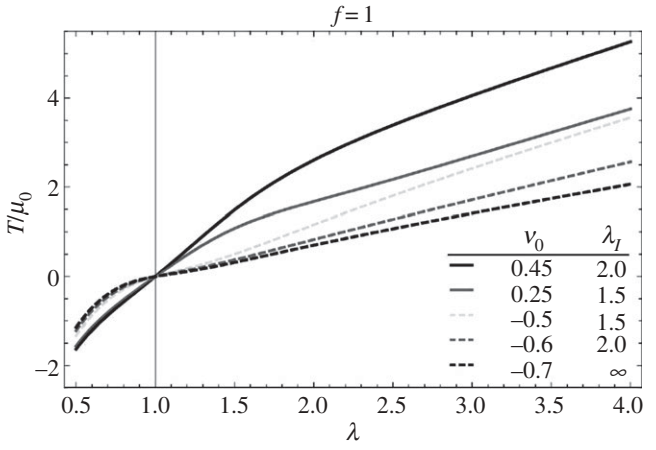

Figure 6. Normalized Cauchy stress T/μ_0 against the stretch λ for $f = 1$ and different values of the constitutive parameters λ_I and ν_0.

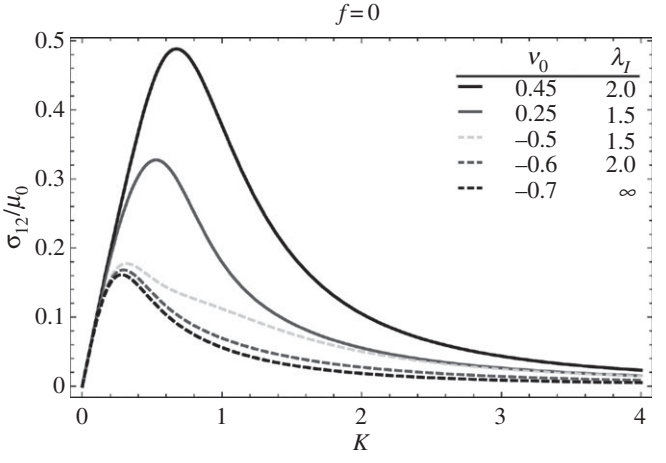

Figure 7. Normalized shear stress σ_{12}/μ_0 against the shear strain K for $f = 0$ and different values of the constitutive parameters λ_I and ν_0.

a lateral expansion (figure 4). In terms of stress, a decrease in the tangent modulus can be seen in figure 6 at large strain. However, for $\lambda_I = \infty$, the microstructure never reaches its limiting state; as such, no increase in the tangent stiffness is seen in the graph.

To further study the behaviour of the proposed model, we consider the deformation given by a simple shear superimposed to a triaxial extension (3.5). By means of equations (3.13) and (2.8), the computation of the normalized shear stress in the case of $f = 0$ gives

$$\hat{\sigma}_{12} := \frac{\sigma_{12}}{\mu_0} = K\frac{\sqrt{1+K^2}}{(1+2K^2)^2}\left\{1-\nu_0\left(\frac{1+2K^2}{\sqrt{1+K^2}}-1\right)\left[1+\pi^2\nu_0^2\left(\frac{1+2K^2}{\sqrt{1+K^2}}-1\right)^2\right]^{-q}\right\}^{-4}, \quad (4.8)$$

which is plotted in figure 7. These stress–stretch curves are similar to those of the Blatz–Ko model: σ_{12} has a non-monotonic behaviour, reaches the maximum of the shear stress and then decreases asymptotically to 0 for increasing K.

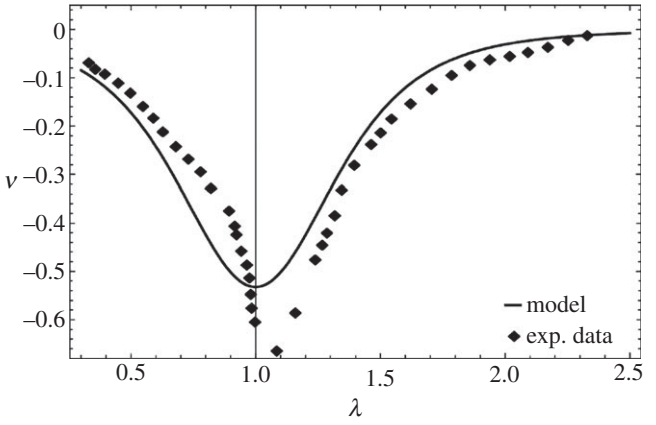

Figure 8. Poisson's function ν in equation (4.1) with the best-fit parameters from table 1 applied to the data in [16].

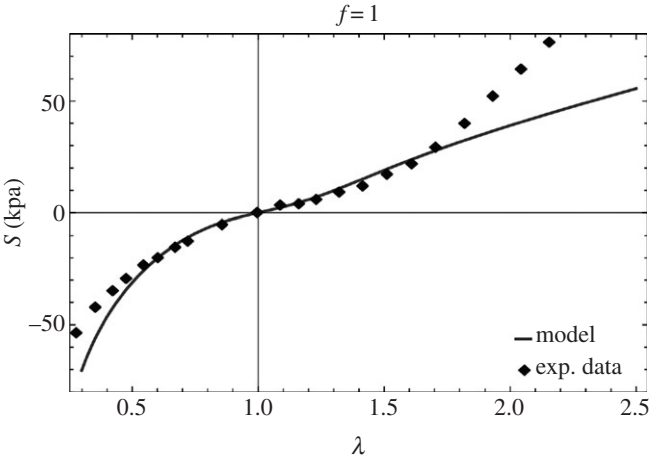

Figure 9. Nominal stress S in terms of the stretch λ with the best-fit parameters from table 1 applied to the data in [16].

5. Experimental data analysis

In this section, we show that the proposed constitutive model is able to describe the large strain behaviour of auxetic foams by presenting fit to data for tension and compression tests on re-entrant foams [16]. These experimental results are, indeed, representative of the mechanical properties of a wide class of auxetic materials [7,17,18].

To avoid the well-known problems inherent to the non-monotonicity of the Blatz–Ko model for $f < 1$ [23], we have set $f = 1$; as a consequence, the constitutive model has only three parameters: μ_0, ν_0 and λ_I.

The expression of the nominal stress S derived from equation (4.6), i.e. $S = \lambda_1^2 T$, was fit against the experimental data by using a nonlinear least-squares method. The fitting results are shown in figure 8 for Poisson's function and in figure 9 for the stress–stretch curve. The identification procedure was performed to match the Poisson function and the stress–stretch curves with the same set of parameters which are listed in table 1. Despite its simplicity, the model is able to match the overall behaviour of the auxetic foam with only three parameters!

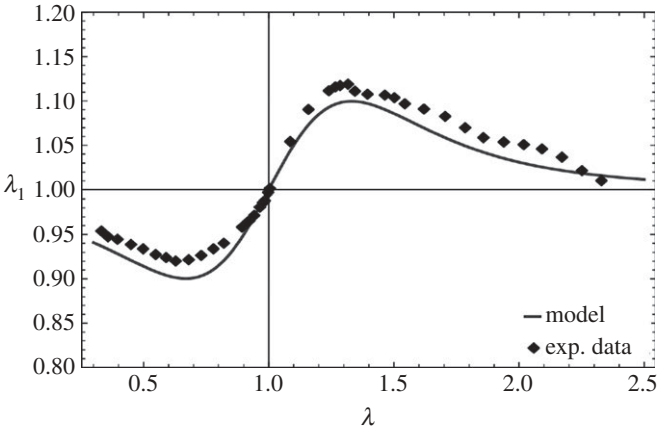

Figure 10. Lateral stretch λ_1 in terms of λ (equation (4.2)) with the best-fit parameters from table 1 applied to the data in [16].

Table 1. Best-fit parameter for the proposed constitutive model ($f = 1$) for data displayed in figures 8–10.

μ_0 (kPa)	ν_0	λ_I
26.53	−0.53	1.33

Poisson's ratio around the undeformed configuration, i.e. $\lambda = 1$, is slightly underestimated by the model, with a predicted value of $\nu_0 = -0.53$ against an experimental value of around -0.62 (figure 8). However, this results in a marginal difference in the lateral stretch λ_1 versus λ curve shown in figure 10. The position of the two maximal values in the experimental curve is matched quite accurately by the model.

For what concerns the stress–stretch curve in figure 9, the model closely follows the experimental data up to 50% of deformation both in tension and compression. At larger stretches, the strain hardening effect seen in the data is not caught by the model. This is not surprising as the model has only one parameter μ_0 and corresponds to a Neo-Hookean hyperelastic model which is well known to display a strain softening behaviour rather than the strain hardening effect seen in the data. Therefore, to accurately fit the data in all the experimental range, a more refined model for the strain energy function W_{12} should be used. However, as structural components, auxetic foams are unlikely to be used in such a large deformation regime.

6. Concluding remarks

The aim of this paper has been to show the possibility of modelling auxetic materials in the framework of the classical theory of nonlinear elasticity. This is possible by using in a suitable way the Poisson function introduced in [12].

The model we propose is feasible for a direct application in a finite-element code and simple as it is based on three constitutive parameters easily identifiable from the experiments: the shear modulus μ_0, the infinitesimal Poisson ratio ν_0 and the lateral stretch at inversion λ_I. The comparison of the model with experimental data confirms a good qualitative agreement with real-world materials. This situation is interesting for several reasons. First of all, we have a mathematical tool to investigate in a simple and direct way the mechanics of auxetic materials at finite strains. Second, the model may be implemented directly in any commercial finite-element software. All this in contrast with complex microstructural-based models that may investigated only via *ad hoc* numerical simulations highly dependent on the specific framework of investigation.

It is clear that the model may be refined in several directions, but its qualitative agreement with the experimental data with only three constitutive parameters is remarkable. We are able to describe the main features of the Poisson function for auxetic materials and to describe stress and strain data over the range of finite strains relevant to the applications.

For all these reasons, we think that it is worth to investigate further this model in various technical applications of auxetic foams where finite deformations cannot be neglected. On the other hand, more refined models could be considered by using a different expression of the strain energy function W_{12}. This is to describe the second-order effects of auxetic foams that may be of a certain interest in specific applications.

We further point out that the procedure we have followed to derive the constitutive model can be generalized to anisotropic materials with the proper choice of the strain energy function W_{12}. This would allow the description of other type of auxetic foams which cannot be considered isotropic owing to the inherent nature of their microstructure.

References

1. Love AEH. 1944 *A treatise on the mathematical theory of elasticity*, p. 643. New York, NY: Dover Publications.
2. Yeganeh-Haeri A, Weidner DJ, Parise JB. 1992 Elasticity of agr-cristobalite: a silicon dioxide with a negative Poisson's ratio. *Science* **257**, 650–652. (doi:10.1126/science.257.5070.650)
3. Baughman RH, Galvao DS. 1993. Crystalline networks with unusual predicted mechanical and thermal properties. *Nature* **365**, 735–737. (doi:10.1038/365735a0)
4. Grima JN, Jackson R, Alderson A, Evans KE. 2000 Do zeolites have negative Poisson's ratios? *Adv. Mater.* **12**, 1912–1918. (doi:10.1002/1521-4095(200012)12:24<1912::AID-ADMA1912>3.0.CO;2-7)
5. Evans KE. 1991 Auxetic polymers: a new range of materials. *Endeavour* **15**, 170–174. (doi:10.1016/0160-9327(91)90123-S)
6. Lakes R. 1987 Foam structures with a negative Poisson's ratio. *Science* **235**, 1038–1040. (doi:10.1126/science.235.4792.1038)
7. Scarpa F, Ciffo LG, Yates JR. 2004 Dynamic properties of high structural integrity auxetic open cell foam. *Smart Mater. Struct.* **13**, 49–56. (doi:10.1088/0964-1726/13/1/006)
8. Bezazi A, Scarpa F. 2007 Mechanical behaviour of conventional and negative Poisson's ratio thermoplastic polyurethane foams under compressive cyclic loading. *Int. J. Fatigue* **29**, 922–930. (doi:10.1016/j.ijfatigue.2006.07.015)
9. Grima JN, Alderson A, Evans KE. 2005 Auxetic behaviour from rotating rigid units. *Phys. Status Solidi (B)* **242**, 561–575. (doi:10.1002/pssb.200460376)
10. Blumenfeld R. 2005 Auxetic strains—insight from iso-auxetic materials. *Mol. Simul.* **31**, 867–871. (doi:10.1080/08927020500295044)
11. Blumenfeld R, Edwards SF. 2012 Theory of strains in auxetic materials. *J. Supercond. Novel Magn.* **25**, 565–571. (doi:10.1007/s10948-012-1464-x)
12. Beatty MF, Stalnaker DO. 1986 The Poisson function of finite elasticity. *J. Appl. Mech.* **53**, 807–813. (doi:10.1115/1.3171862)
13. Murphy JG. 2000 Strain energy functions for a Poisson power law function in simple tension of compressible hyperelastic materials. *J. Elast.* **60**, 151–164. (doi:10.1023/A:1010843015909)
14. Murphy JG, Rogerson G. 2002 A method to model simple tension experiments using finite elasticity theory with an application to some polyurethane foams. *Int. J. Eng. Sci.* **40**, 499–510. (doi:10.1016/S0020-7225(01)00079-9)
15. Blatz PJ, Ko WL. 1962 Application of finite elastic theory to the deformation of rubbery materials. *Trans. Soc. Rheol.* **251**, 223–251. (doi:10.1122/1.548937)
16. Choi JB, Lakes RS. 1992 Non-linear properties of polymer cellular materials with a negative Poisson's ratio. *J. Mater. Sci.* **27**, 4678–4684. (doi:10.1007/BF01166005)
17. Prall D, Lakes RS. 1997 Properties of a chiral honeycomb with a Poisson's ratio of −1. *Int. J. Mech. Sci.* **39**, 305–314. (doi:10.1016/S0020-7403(96)00025-2)
18. Ugbolue SC, Kim YK, Warner BS, Fan Q, Chen-Lu Y, Kyzymchunk O, Lord J. 2012 Engineered warp knit auxetic fabrics. *J. Textile Sci. Eng.* **2**, e103. (doi:10.4172/2165-8064.1000e103)

19. Batra RC. 1976 Deformation produced by a simple tensile load in an isotropic elastic body. *J. Elast.* **6**, 109–111. (doi:10.1007/BF00135183)
20. Truesdell CA, Noll W. 1965 Chapter D, Section 51. In *The non-linear field theories of mechanics* (ed. SS Antman), 3rd edn., p. 627. Berlin, Germany: Springer.
21. Wineman AS, Waldron WK. 1995 Normal stress effects induced during circular shear of a compressible non-linear elastic cylinder. *International J. NonLinear Mech.* **30**, 323–339. (doi:10.1016/0020-7462(94)00043-A)
22. Lakes R. 1991 Deformation mechanisms in negative Poisson's ratio materials—structural aspects. *J. Mater. Sci.* **26**, 2287–2292. (doi:10.1007/BF01130170)
23. Horgan CO. 1996 Remarks on ellipticity for the generalized Blatz–Ko constitutive model for a compressible nonlinearly elastic solid. *J. Elast.* **42**, 165–176. (doi:10.1007/BF00040959)